**Subscripts**

$a$ = ambient
$f$ = moving front
$f1$ = moving front no. 1
$f2$ = moving front no. 2
$fi$ = $i$-th moving front
$fj$ = moving front closest to $X = 0$
$h$ = hydrocarbon
$i$ = region $i$ or $i$-th isotherm
$j$ = region $j$ or in the region closest to $X = 0$
$l$ = liquid
$m$ = isotherm closest to $X = 1$
$o$ = initial temperature
$s$ = at complete solidification
$w$ = water

**Superscripts**

$n$ = $n$-th time step

**LITERATURE CITED**


Carslaw, H. S., and J. C. Jaeger, "Conduction of Heat in Solids," Chap. XI, Clarendon Press, Oxford (1959).

Chernous'ko, F. L., "Solution of Non-Linear Heat Conduction Problems in Media with Phase Change," *Int. Chem. Eng.*, **10**, 42 (1970).

Crank, J., and R. D. Pahle, "Melting Ice by Isotherm Migration Method," *Bull. J. Inst. Maths. Applics.*, **9**, 12 (1973).

Crank, J., and R. S. Gupta, "Isotherm Migration Method in Two Dimensions," *Int. J. Heat Mass Transfer*, **18**, 1101 (1975).

Dix, R. C., and J. Cizek, "The Isotherm Migration Method for Transient Heat Conduction Analysis," Proc. Fourth Int'l Heat Transfer Conference, Paris, **1**, ASME New York (1971).

Jefferson, T. B., O. W. Witzell and W. L. Sibit, "Thermal Conductivity of Graphite-Silicone Oil and Graphite-Water Suspensions," *Ind. Eng. Chem.*, **50**, 1589 (1958).

Kreith, F., *Principles of Heat Transfer*, 3rd ed. IEP, New York (1973).

Schneider, P. J., *Conduction Heat Transfer*, Addison-Wesley, Cambridge, MA (1955).

Shamsundar, N., "Comparison of Numerical Methods for Diffusion Problems with Moving Boundaries," *Moving Boundary Problems*, D. G. Wilson, A. D. Solomon, and P. T. Boggs, eds., p. 165, Academic Press, New York (1978).



*Manuscript received July 25, 1980; revision received December 8, and accepted January 20, 1981.*


# Modeling of Three Phase Reactors: A Case of Oxydesulfurization of Coal


**J. B. JOSHI**

**J. S. ABICHANDANI**

**and**

**Y. T. SHAH**

**Department of Chemical and Petroleum Engineering**
**University of Pittsburgh**
**Pittsburgh, PA**

**and**

**J. A. RUETHER**

**and**

**H. J. RITZ**

**Pittsburgh Energy Technology Center**
**U.S. Department of Energy**
**Pittsburgh, PA 15213**



**Mathematical models have been developed for the design of bubble column slurry reactors, wherein the solids take part in the reaction and follow the shrinking core model. The cases of liquid film control, ash diffusion control, and chemical reaction control have been analyzed. Experiments were performed in a 22.2 mm i.d. continuous cocurrent bubble column slurry reactor for the removal of pyritic sulfur by oxidation from aqueous slurries of Upper Freeport, Lower Freeport, Kentucky No. 9, and Pittsburgh seam coals, in the temperature range of 430-480°K at 6.8 MPa total pressure. The theoretical predictions are found to be in good agreement with experimental results.**


## SCOPE

Bubble column slurry reactors are very popular in industry situations where the solids either take part in the reaction or act as catalyst. In this investigation, solids that do not change particle size during the reaction are investigated. The performance of such reactors will depend upon interphase, inter- and intra-particle mass and heat transfer, and the intrinsic chemical kinetics. It is well known that backmixing is detrimental to the conversion. Using dispersion models, earlier studies have accounted for the extent of backmixing. However, for situations where solids take part in a reaction that is described by nonlinear rate equations, the dispersion models are not applicable and it is necessary to develop models based on the exit age distributions.

In an application of the models, experiments were performed on the removal of pyritic sulfur from coal by oxidation with air in a continuous bubble column slurry reactor. The effects of temperature, reaction time, and superficial gas velocity were investigated. Some scale-up considerations are examined.

## CONCLUSIONS AND SIGNIFICANCE

**Factors influencing the performance of bubble column slurry reactors include gas-liquid mass transfer, liquid-solid mass transfer, intraparticle diffusion, adsorption, surface reaction, and desorption of the products. Any one or more of the above resistances could be the rate-controlling steps. This as well as nonlinear kinetics and nonuniform particle size makes the system highly complicated for most practical applications.**

**In this work, the shrinking core mechanism is used to analyze the case of unchanging particle size. The rate-controlling mechanisms of liquid-solid mass transfer, diffusion through the product ash layer, and the surface reaction are considered separately. The solid phase backmixing was accounted for on the basis of the exit age distribution. Performance charts for all the controlling mechanisms have been presented in the form of average conversion of the solid phase in relation to the parameters of the average residence time, the solid phase Peclet number, and the time required for complete conversion of a single particle. These charts should be useful for the design of such reactors.**

**Experiments in a continuous bubble column slurry reactor indicate that more than 95% of the pyritic sulfur can be removed in the temperature range of 450-475°K, average residence time of 1800 s, and solid phase Peclet number range of 2-5. On the basis of time required for complete conversion, obtained from batch reactor experiments, a fairly good agreement was found between the model prediction and the experimental results from the continuous bubble column slurry reactor.**

## INTRODUCTION

There are several industrially important gas-liquid-solid reactions, such as coal liquefaction, carbonation of lime, bio-oxidation of suspended organic solids, and production of gas hydrates, where solids take part in the reaction. The common type of reactor for these reactions is gas-liquid-suspended solid columns with or without mechanical agitation. An extensive literature is available on the hydrodynamic, mixing, mass transfer, and heat transfer characteristics of three phase reactors, and critical reviews have been published in recent years (Shah, 1979; Choudhari and Ramchandran, 1980).

The mechanism with which the solids react depends upon the specific case. In general, the reactions may be classified into two broad categories, one in which the solids change their particle size and the other in which the particle size is retained. Coal liquefaction, carbonation of lime, oxidation of calcium sulfite, and production of acetylene by the reaction between calcium carbide and water fall in the first category.

For cases in the second category, the rate-controlling step can be gas-liquid mass transfer, liquid-solid mass transfer, diffusion through product ash layer, chemical reaction, or the combination of two or more steps. These problems can often be analyzed on the basis of the "Shrinking Core Model" (Levenspiel, 1972). The experimental work reported here, the oxidation of iron pyrite by dissolved oxygen in aqueous solution, falls in the second category.

In addition to mass transfer and chemical reaction, the performance of three-phase reactors depends upon the hydrodynamic (phase holdups and their variation) and the mixing characteristics of the reactor. The problem is further aggravated because of the different extents of micromixing and segregation in all the three phases. Govindarao (1975) has developed a mathematical model under steady-state and transient conditions for three-phase slurry reactors. Parulekar and Shah (1980) considered the variations in the gas and liquid velocities and the total pressure. In both of these cases, the solids acted as a catalyst, and the rate was proportional to solid loading. Where solids take part in the reaction, the rate equation can be nonlinear (other than first order), and then the extent of segregation in the solid phase becomes important.

In the present work, mathematical models and reactor performance charts for cases where the solids take part in the reaction and follow the shrinking core mechanism are developed. Ruether (1979) has analyzed the problem for completely backmixed stirred tanks in series for the diffusion-controlled mechanism. The differential mode of operation and three controlling mechanisms are considered in the present work.

Sulfur exists in coal in two main forms. Organic sulfur is chemically bonded to the organic matrix. Pyritic sulfur is present in the form of crystals, agglomerations of crystals called framboids, and in other more massive forms. The pyritic sulfur prevails as a distinctly different phase in the organic coal matrix. A number of methods are under investigation for the precombustion removal of sulfur from coal by selective oxidation or reduction (Meyers, 1977). In general the methods achieve a higher conversion of pyritic than organic sulfur. The objective is to reduce the sulfur content to the point where the coal may be burned without the need for a post-combustion cleanup step such as scrubbers to remove sulfur oxides.

One approach to chemical coal cleaning treats an aqueous slurry of coal with purified oxygen or air at elevated temperature and pressure. This method is known as "oxydesulfurization." Alkalies such as sodium carbonate or ammonia may also be added to the liquid. In the absence of added alkali the aqueous medium is acidic, since the principal product for converted sulfur is sulfuric acid. Under alkaline conditions workers at Ames National Laboratory have shown the rate controlling step for pyrite oxidation is diffusion of oxygen through the product $Fe_2O_3$ layer (Greer et al., 1980; Chuang et al., 1980). They correlated their results using the shrinking core model. Recently Joshi et al. (1980) studied the effects of temperature, oxygen partial pressure, and coal particle size on the rate of pyrite oxidation under acidic conditions. The data indicated the shrinking core model again applied, with the rate determining step for these conditions being chemical reaction between pyrite and dissolved oxygen.

In this paper we report process development work for oxydesulfurization of coal under acidic conditions. The work was conducted in a 22.2 mm i.d. bubble column slurry reactor for coals from several different seams, varying temperature, oxygen partial pressure, and slurry residence time. The experimentally observed conversion of pyrite is compared to the model predictions.

## MATHEMATICAL MODEL

In a three phase gas-liquid-solid system, the overall rate may be controlled by one or more steps, namely gas-liquid mass transfer, diffusion through the product ash layer and chemical reaction. Here we consider only those cases in which the solid phase contributes to the rate controlling step. At the beginning a generalized case will be considered, and the results will then be applied to the specific case of the oxydesulfurization of coal.

Consider the following reaction occurring in spherical particles:

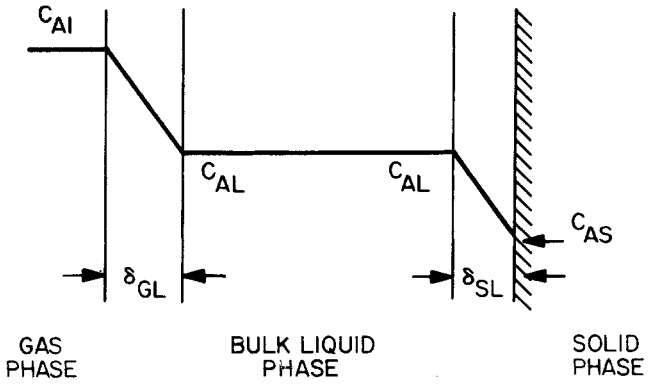


Figure 1. Typical concentration profile for gas-liquid-solid system.

$$A(\text{fluid}) + bB(\text{solid}) \rightarrow \text{Products} \quad (1)$$

For the case of oxydesulfurization, $A$ is oxygen and $B$ is pyrite.

The possible reactions during the oxidation of pyrite are (McKay and Halpern (1958)):

$$FeS_2 + 2O_2 \rightarrow FeSO_4 + S \quad (2a)$$

$$2S + 3O_2 + 2H_2O \rightarrow 2H_2SO_4 \quad (2b)$$

$$FeS_2 + 3.5O_2 + H_2O \rightarrow FeSO_4 + H_2SO_4 \quad (2c)$$

$$FeS_2 + 3.75O_2 + \tfrac{1}{2} H_2O \rightarrow Fe_2(SO_4)_3 + \tfrac{1}{2} H_2SO_4 \quad (2d)$$

$$FeS_2 + 3.75O_2 + 2H_2O \rightarrow \tfrac{1}{2} Fe_2O_3 + 2H_2SO_4 \quad (2e)$$

Vracar and Vucurovic (1970) reported that reaction (Eq. 2a) does not proceed at temperatures above 413°K. This agrees with the work of Biernat and Robins (1969) who concluded on the basis of potential—pH diagrams for the Fe-S-$H_2O$ system that the S species is unstable above a temperature of 425°K. The lowest temperature employed in the work reported on here was 443°K. The product distribution of the pyrite oxidation reaction under equilibrium conditions has been reported by Peters (1973). In the range of pH encountered in this work, the possible products are hematite ($Fe_2O_3$) and iron sulfates. X-ray diffraction tests conducted in our laboratory of the solid reaction products of the oxydesulfurization of pyrite under acidic conditions indicates the principal iron-containing product is iron oxide. Therefore in the present work Eq. 2e was used for the stoichiometry of the reaction.

The steps during the oxidation of pyrite in slurry are as follows (Figure 1):

(1) Dissolution of solute gas in the liquid phase. The rate is given by

$$R_A = k_L a\{C_{AI} - C_{AL}\} \quad (3)$$

(2) Transfer of solute gas from liquid phase to the solid surface. The rate is given by (Figure 2)

$$R_A = k_{SL} a_p\{C_{AL} - C_{AS}\} \quad (4)$$

(3) Diffusion of solute gas through the product ash layer (Figure 3)

(4) Chemical reaction (Figure 4)

The following assumptions will be made:

(1) The variations in total pressure due to the static head of liquid are small as compared to the total pressure.

(2) The conversion of solute in the gas phase is small. Therefore, the extent of backmixing in the gas phase is unimportant. The interfacial concentration of the solute gas will be calculated at the log mean partial pressure between the inlet and the outlet.

(3) As a consequence of assumptions 1 and 2, the superficial gas velocity, the gas holdup, and the liquid solid mass transfer coefficient remain practically constant along the length of the reactor.

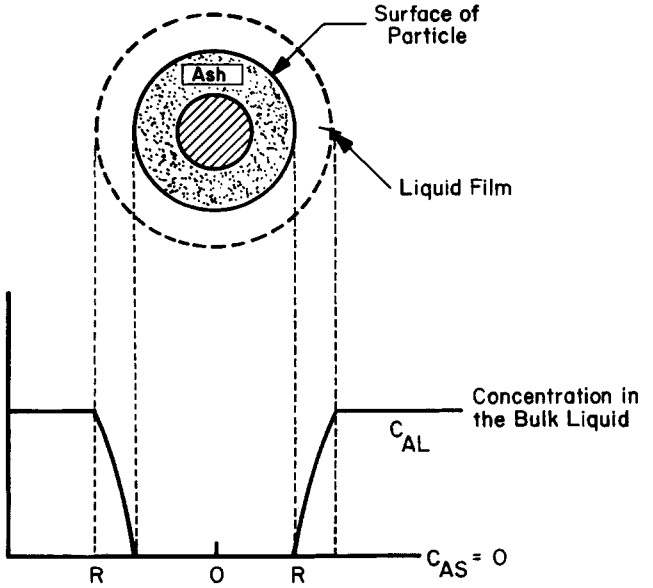


Figure 2. Representation of a reacting particle when diffusion through the liquid film is the controlling resistance.

(4) The solid loading is uniform in the reactor. This assumption is reasonable when the particle size is small (<100 microns) and/or the density difference between the solid and liquid is small.

(5) The overall reaction will be assumed to be controlled by a single step.

(6) Since the particles retain their identity in the reactor and since the rate equations are nonlinear, the usual dispersion model cannot be applied for the present case in so far as the conversion of a particular chemical species is concerned. Therefore, a residence time distribution model will be used. Kato et al. (1972) have shown that the residence time distribution (RTD) of the solid phase can be represented by the "diffusion-sedimentation" model. This model considers the fact that the RTD of the liquid and the solid phases will be identical if the particle settling velocity is zero. In the present case of fine

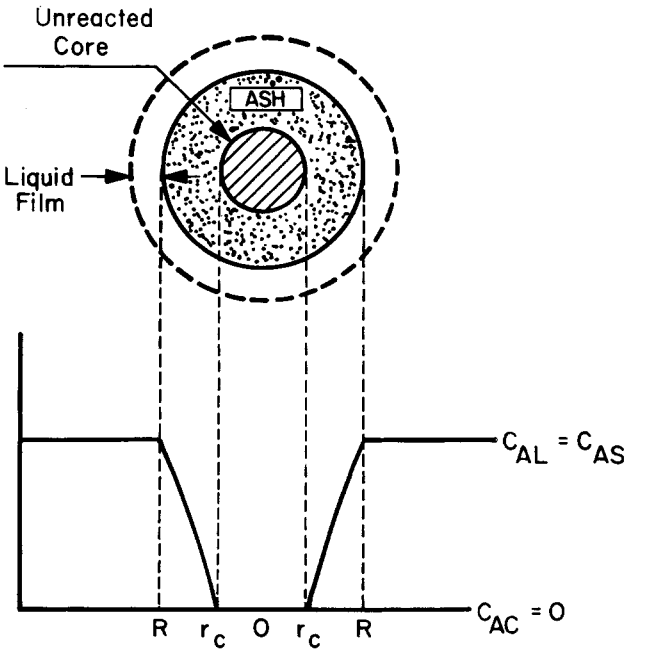


Figure 3. Representation of a reacting particle when diffusion through ash layer is the controlling resistance.

pyrite particles (<100 microns) it will be assumed that the axial dispersion coefficient for the solid and the liquid phases are the same. The experimental results of Kato et al. (1972) support this assumption. Therefore, the exit age distribution of the solid particles will be found by following the same procedure as for the liquid phase. The exit age distribution of particles is assumed to be the same as the response to an impulse input.

The governing equations are

$$\frac{\partial C}{\partial \theta} = \frac{1}{\text{Pe}} \frac{\partial^2 C}{\partial Z^2} - \frac{\partial C}{\partial Z} \tag{5}$$

where

$$\theta = \frac{t \cdot V_{SL}}{L(1 - \epsilon_G)} \tag{6}$$

$$Z = z/L \tag{7}$$

and

$$\text{Pe} = \frac{LV_{SL}}{\epsilon_{SL} D_{SL}} = \frac{LV_S}{\epsilon_S D_S} \tag{8}$$

The boundary conditions are

$$C_{in} = C - \frac{1}{\text{Pe}} \frac{\partial C}{\partial Z} \text{ at } Z = 0; \text{ all } \theta \tag{9}$$

$$\frac{\partial C}{\partial Z} = 0 \text{ at } Z = 1; \text{ all } \theta \tag{10}$$

$$C = 0 \text{ at } \theta = 0; \text{ all } Z \tag{11}$$

The parameters are

$$\int_0^\infty C \, dt = \int_0^\infty \frac{c}{Q} \, dt = 1 \tag{12}$$

and

$$Q = \int_0^\infty c \, d \, t \tag{13}$$

where $c$ is the actual concentration at the exit.

Mecklenburgh and Hartland (1975) have solved Eqs. 5-13 and the exit age distribution in dimensionless form is

$$E(\theta) = 2 \exp(\text{Pe}/2) \sum_{r=1}^{\infty} (-1)^{r+1} \exp(T_r \theta) \frac{b_r^2}{\frac{4}{\text{Pe}} + 1 + b_r^2} \tag{14}$$

where $b_r$ is the root of

$$b_r = \tan\left(r\frac{\pi}{2} - \frac{\text{Pe} b_r}{4}\right) \tag{15}$$

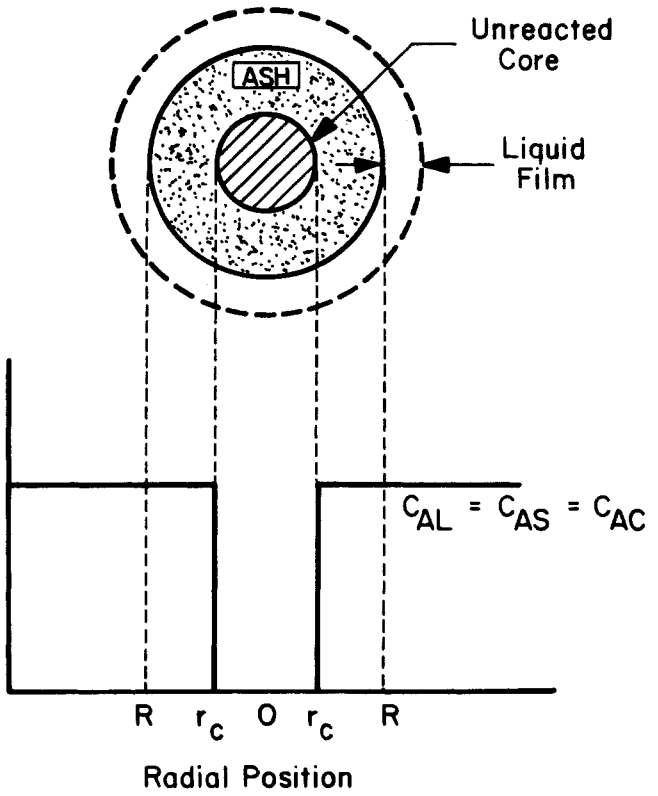


**Figure 4. Representation of a reacting particle when chemical reaction is the controlling resistance.**

TABLE 1. EIGEN VALUES OF EQ. 14

| | Pe = 0.1 | | Pe = 0.5 | | Pe = 1 | | Pe = 5 | |
|---|---|---|---|---|---|---|---|---|
| $r$ | $b_r$ | $T_r$ | $b_r$ | $T_r$ | $b_r$ | $T_r$ | $b_r$ | $T_r$ |
| 1. | 6.31 | −1.02 | 2.77 | −1.087 | 1.92 | −1.17 | 0.74 | −1.94 |
| 2. | 63.5 | −100.87 | 13.18 | −21.85 | 6.87 | −12.04 | 1.68 | −4.80 |
| 3. | 126.1 | −397.28 | 25.46 | −81.16 | 12.88 | −41.75 | 2.79 | −10.98 |
| 4. | 188.8 | −891.24 | 37.93 | −179.96 | 19.07 | −91.16 | 3.96 | −20.94 |
| 5. | 251.6 | −1582.75 | 50.45 | −318.27 | 25.3 | −160.32 | 5.18 | −34.81 |
| 6. | 314.4 | −2471.81 | 62.99 | −496.08 | 31.56 | −249.22 | 6.41 | −52.61 |
| 7. | | | 75.54 | −713.40 | 37.82 | −357.89 | 7.65 | −74.35 |
| 8. | | | 88.10 | −970.23 | 44.09 | −486.3 | 8.89 | −100.04 |
| 9. | | | | | 50.37 | −634.48 | 10.13 | −129.68 |
| 10. | | | | | 56.64 | −802.40 | 11.38 | −163.23 |
| 11. | | | | | | | 12.63 | −200.8 |
| 12. | | | | | | | 13.87 | −242.3 |
| 13. | | | | | | | 15.14 | −287.7 |
| 14. | | | | | | | 16.39 | −337.1 |
| 15. | | | | | | | 17.65 | −390.5 |
| 16. | | | | | | | 18.90 | −447.8 |
| 17. | | | | | | | 20.15 | −509.0 |
| 18. | | | | | | | 21.41 | −574.2 |
| 19. | | | | | | | 22.66 | −643.3 |
| 20. | | | | | | | 23.91 | −716.4 |

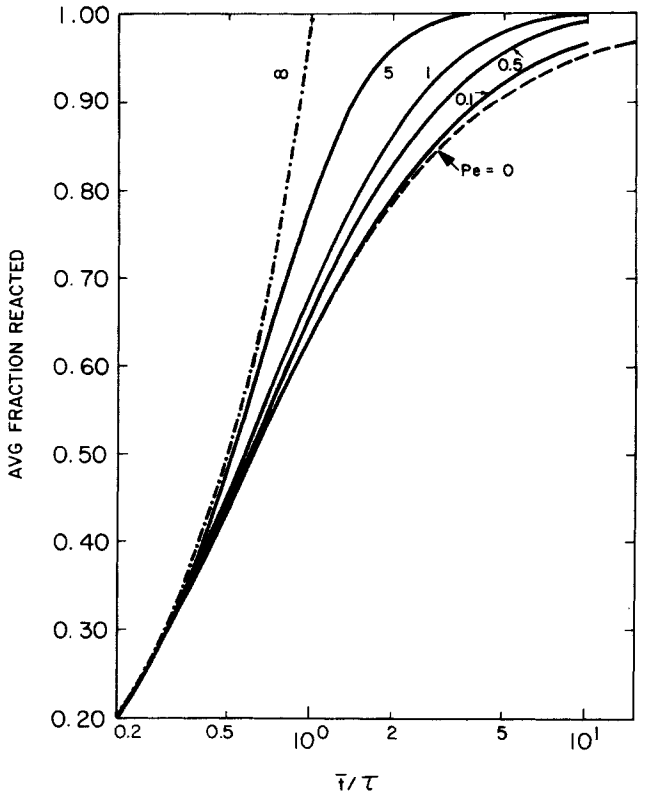


Figure 5. Performance chart: external mass transfer controlled mechanism.

and

$$T_r = \left(-\frac{\text{Pe}}{4}\right)(1 + b_r^2) \tag{16}$$

(7) The particles are spherical and of uniform size. The problem of size distribution will be analyzed later.
(8) The reactor is isothermal.

#### Case 1: Liquid Solid Mass Transfer Controlled

For this case, the relationship between time and fractional conversion is given by the following equation (Levenspiel, 1972).

$$\frac{t}{\tau} = x \tag{17}$$

where

$$\tau = \frac{\rho_B R}{3bk_{SL}C_{AL}} \tag{18}$$

Equation 17 also holds for the case of a plug-flow reactor where $t$ is the residence time.

For the case of continuous feed of particles to a bubble column slurry reactor, having an exit age distribution of particles $E(t)$, a mass balance gives

$$1 - X = \int_0^\tau (1 - x)\, E(t)\, dt \tag{19}$$

Equation 19 can be written in the following dimensionless form:

$$1 - X = \int_0^{\tau/\bar{t}} (1 - x)\, E(\theta)\, d\theta \tag{20}$$

where $E(\theta)$ is given by Eq. 14. Equation 20 was integrated with the help of Eqs. 14-16 and 17-18. The stepwise procedure is given below:

(1) The average overall conversion depends upon Peclet number (Pe), the time required for complete conversion ($\tau$) and the average residence time ($\bar{t}$). Select a suitable set of values for Pe, $\tau$ and $\bar{t}$.

(2) For the numerical integration of Eq. 20, a suitable value of the time increment ($\Delta t$) is required. The accuracy of the numerical integration depends upon $\Delta t$. Its value was selected when the difference between the consecutive results was less than 0.1 percent when $\Delta t$ was halved for the successive calculations.

(3) Starting at $t = 0$, calculate $\theta = t/\bar{t}$

(4) At a given time, it is necessary to find fractional conversion ($x$) and $E(\theta)$. The value of ($x$) was obtained from Eq. 17. The value of $E(\theta)$ can be obtained from Eq. 14 if the eigenvalues $b_r$ and $T_r$ are known. For this purpose, Eqs. 15 and 16 were solved and the results are summarized in Table 1. The tabulated values are sufficient for 0.1 percent accuracy for the respective values of Peclet numbers.

(5) Use $x$ and $E(\theta)$ for the integration of Eq. 20. Integrate up to $\tau/\bar{t}$ to get the fraction unreacted.

(6) Repeat Eqs. 1-5 to cover a wide range of Pe, $\tau$ and $t$. The results are shown in Figure 5.

The fractional conversion for the case of a completely backmixed reactor (Pe = 0) can be obtained if $E(\theta)$ is given by the following equation:

$$E(\theta) = e^{-\theta} \tag{21}$$

Substitution of Eqs. 17 and 21 in Eq. 20 gives (Levenspiel, 1972)

$$X = \frac{\bar{t}}{\tau}(1 - e^{-\tau/\bar{t}}) \tag{22}$$

Equation 22 is also plotted in Figure 5.

The fractional conversion for the plug flow reactor (Pe = ∞) will be the same as the semi-batch reactor under otherwise

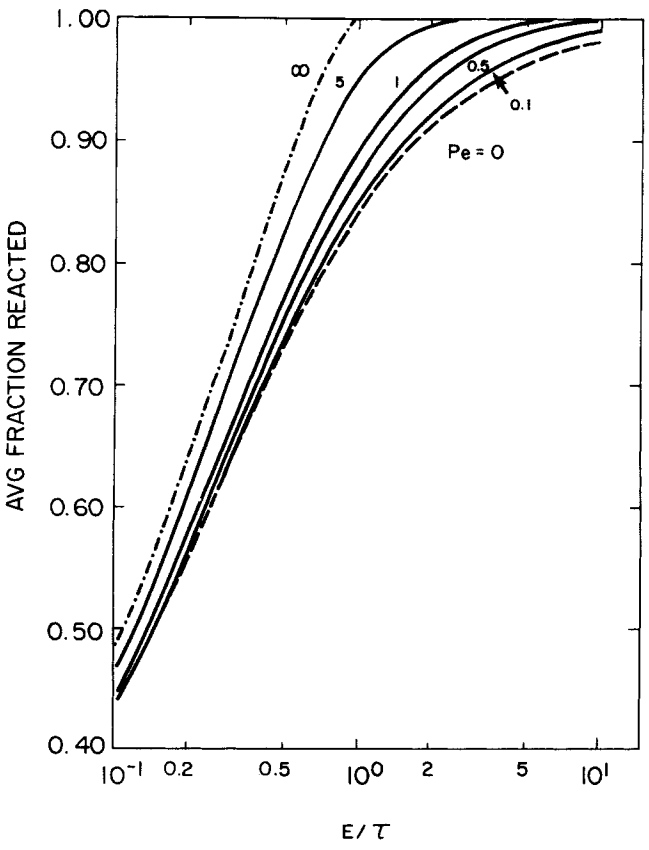


Figure 6. Performance chart: ash diffusion controlled mechanism.

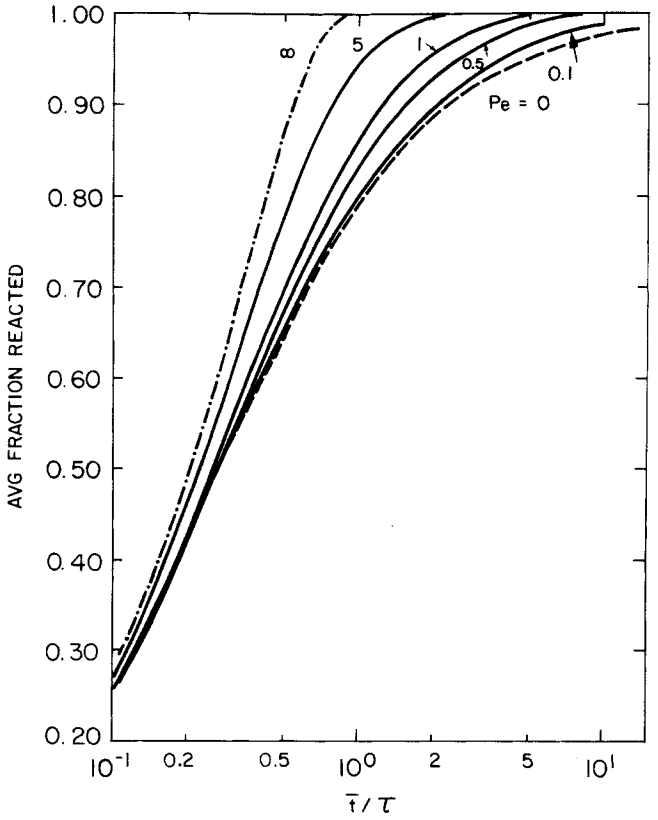


**Figure 7. Performance chart: chemical reaction controlled mechanism.**

identical conditions. Therefore, Eq. 17 is plotted in Figure 5 for the prediction of a plug-flow reactor.

#### Case 2: Ash Diffusion Controlled

The relationship between time and fractional conversion is given by Levenspiel (1972) (Figure 3)

$$\frac{t}{\tau} = 1 - 3(1 - x)^{2/3} + 2(1 - x) \tag{23}$$

where

$$\tau = \frac{\rho_B R^2}{6bD_e C_{AS}} \tag{24}$$

For the case of a completely backmixed reactor, the fractional conversion is given by the following equation (Levenspiel, 1972)

$$X = 1 - \frac{\tau}{5\bar{t}} + \frac{19}{420}\left(\frac{\tau}{\bar{t}}\right)^2 - \frac{41}{4620}\left(\frac{\tau}{\bar{t}}\right)^3 + 0.00149\left(\frac{\tau}{\bar{t}}\right)^4 \tag{25}$$

Using the same procedure as in Case 1, the average fractional conversion was obtained as a function of Pe, $\tau$ and $\bar{t}$. Equation 23 gives the predictions of a plug flow reactor. The results are given in Figure 6.

#### Case 3: Chemical Reaction Controlled

For this case (Figure 4)

$$\frac{t}{\tau} = 1 - (1 - x)^{1/3} \tag{26}$$

where

$$\tau = \frac{\rho_B R}{bk_r C_{AS}} \tag{27}$$

for reaction first order in component A.

For the case of completely backmixed reactor (Levenspiel, 1972)

$$X = 3\frac{\bar{t}}{\tau} - 6\left(\frac{\bar{t}}{\tau}\right)^2 + 6\left(\frac{\bar{t}}{\tau}\right)^3 (1 - e^{-\tau/\bar{t}}) \tag{28}$$

For the predictions of a plug-flow reactor, Eq. 26 was used. Figure 7 shows the fractional conversion as a function of Pe, $\tau$ and $t$.

From Figures 5-7 it can be seen that the curves shift progressively from plug flow (Pe = ∞) towards completely backmixed reactor (Pe − 0). It may be noted that the performance of the plug flow and completely backmixed reactors is given by the closed form equations.

As expected, for any particular $t/\tau$, the conversion increases with increase in Pe, or conversely, the time required to attain a particular level of conversion is lower for higher Peclet numbers.

Our results show that this type of analysis is of significance between Peclet numbers of 0.2 and 5, as beyond these limits, the difference in the levels of conversion for the extreme cases of plug flow and completely backmixed reduces to less than 10%.

Ruether (1979) reported a performance chart for the case of ash diffusion controlled reaction in $N$ completely backmixed reactors in series. A comparison can be made between results obtained using that approach and the one developed here. This was done by equating the variances for the stirred tanks in series model and the dispersed plug flow model according to (Levenspiel and Bischoff, 1963)

$$\frac{1}{N} = \frac{2}{\text{Pe}} - \frac{2}{\text{Pe}^2}(1 - \exp(-\text{Pe}))$$

Satisfactory agreement between the two models was obtained over the range of reduced times and Peclet numbers shown in Figure 6. It is noted that the abscissa in Figure 1 of Ruether's paper should read $N\ V_l b\ C_A\ D_e/F\ \rho_B R^2$.

## EXPERIMENTAL

### Materials

Experiments were performed using four coals, namely Upper Freeport, Lower Freeport, Kentucky No. 9 and Pittsburgh. Samples of coal were obtained directly from the mines in 55 gallon drums. These samples were air dried, pulverized, and prepared according to ASTM method D-346. A representative sample of each drum of prepared coal was analyzed to determine the ultimate and proximate analyses, Btu content and sulfur forms.

### Apparatus

The bubble column slurry reactor consisted of a titanium tube, 22.2 mm i.d. by 1829 mm long, with 1.65 mm wall thickness. Coal-slurry was prepared in an agitated vessel $V_1$ hung from a weigh scale with electronic readout. Slurry was drawn from $V_1$ and circulated in a loop by an advancing cavity pump. A slip stream from the circulation loop was fed to a high pressure piston pump. This pump injected slurry through a coiled preheater and into the bottom of the reactor. Compressed air was also fed to the reactor, and its rate was monitored by rotameter. The air passed through a coiled tube preheater and entered the bottom of the reactor via a nozzle having five 0.08 mm holes. Column and preheaters were heated electrically, the temperatures were controlled by proportional controllers. Temperature was measured at three axial positions inside the reactor by a thermocouple probe inserted from the top of the reactor tube. Pressure was measured by a Bourdon tube gauge. The effluent gas-slurry mixture was cooled in a heat exchanger and then passed to one of two lock hoppers, $V_2$, where the gas and slurry was disengaged. Effluent gas passed from $V_2$ through

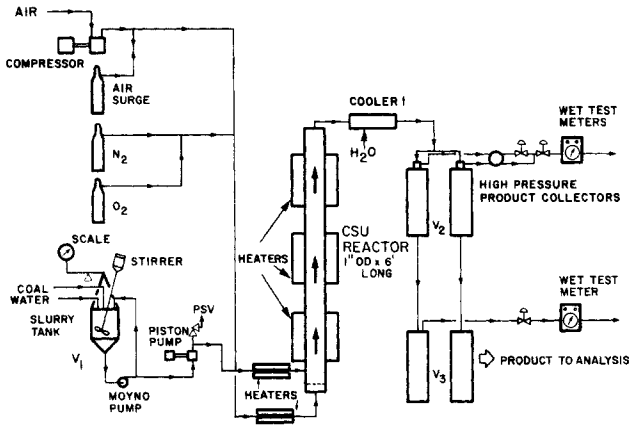


Figure 8. Experimental apparatus.

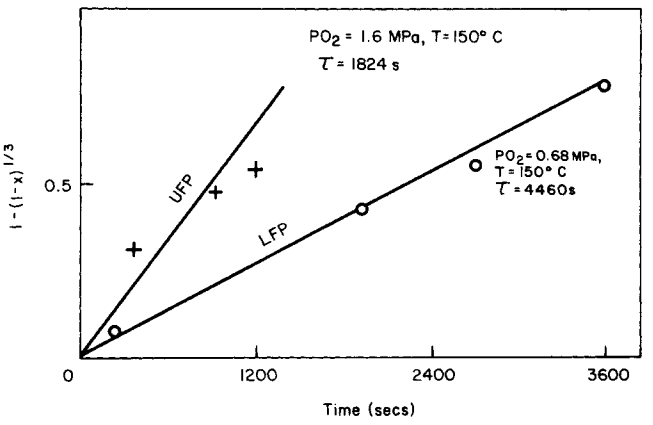


Figure 9. Results from semibatch reactor for the oxidation of pyrite from Upper (UFP) and Lower Freeport (LFP) coals.

a back pressure regulator and finally through a wet test meter before being vented. The experimental apparatus is shown in Figure 8.

### Procedure

Batches of coal-water slurry were prepared using only coal and tap water. The batches were calculated to contain 26.0% moisture-free coal. The coal-water slurry was charged to vessel $V_1$. Solids were kept in suspension through the help of a stirrer and by recirculation. Vessel $V_1$ had a conical bottom, preventing the occurrence of dead spots.

At the start of the experiment, the system was filled with tap water. Preheated slurry and air were then introduced to the reactor at predetermined flow rates. The average apparent residence time ($t'$) was calculated on the basis of total column volume and the slurry flow rate. The time was taken to be zero when the temperature, total pressure, and the flow rates reached the prescribed levels. Steady-state conditions were assumed to prevail after $5t'$. The time equivalent to the subsequent $3t'$ was used to collect the operating data.

Pressure in the system was controlled by a back pressure regulator downstream from the product collector $V_2$. Temperature fluctuation at any axial position in the reactor did not exceed 3°K. Lock hoppers $V_2$ accumulated product samples. Each of the five unsteady-state and three steady-state samples were initially accumulated in $V_2$ and then collected in $V_3$, a plastic container. Each sample collected weighed approximately 0.75 kg. Each steady-state sample was weighed, filtered, and dried at 305°K until the 24 hour weight loss was equal to or less than 3.5%. The samples were then pulverized, riffled, and analyzed. The results of the three steady-state samples were averaged for final results. Each sample was analyzed for sulfur forms, total sulfur, and heating value; and proximate and ultimate analyses were performed. The exit gas was analyzed for CO, $CO_2$, $O_2$, $N_2$, and hydrocarbons. Carbon monoxide and hydrocarbons were not found.

## RESULTS AND DISCUSSION

### Semi-Batch Experiments to Determine Rate Expression for Oxidation of Pyrite Particles

For modeling continuous three phase oxydesulfurization reactors, it is necessary to have a rate expression for pyrite oxidation in terms of temperature and composition of the aqueous phase surrounding a particle. For this purpose an experimental program was undertaken using Lower Freeport seam coal in a stirred semi-batch reactor (batchwise charge of slurry, continuous flow of air). The temperature and oxygen partial pressure were varied in the range 430-475°K and 0.32-1.36 MPa, respectively. Narrow sized cuts of coal particles in the ranges 0 × 72, 72 × 99, 150 × 208, 208 × 430, and 700 × 1400 microns were used. The pyrite particle size distribution was determined for each of the sized cuts of coal. It was found that most of the pyrite (by weight) existed in a liberated form, as opposed to being incased in coal particles. Average pyrite particle sizes were computed for each sized cut of coal. These are shown in Table 2. Data for the oxidation of pyrite were used to develop a rate expression (Joshi et al., 1980), and the results are briefly reviewed here. Rate was independent of stirrer speed and slurry concentration, indicating gas absorption resistance was negligible. Calculations showed that external particle/liquid mass transfer resistance was also negligible. Rate increased with oxygen partial pressure to the 0.7 power.

TABLE 2. PYRITE PARTICLE SIZE DISTRIBUTION IN COAL

| Pyrite Size Category, Microns | Coal Size, Microns | | | | |
|---|---|---|---|---|---|
| | 72×0 | 72×99 | 150×208 | 208×430 | 700×1410 |
| | Weight Percent of Size in Microns | | | | |
| 0-6 | 0.26 | 0.01 | 0.04 | — | — |
| 6-12 | 2.30 | 0.15 | 0.17 | — | — |
| 12-24 | 9.38 | 0.99 | 1.27 | 0.08 | 0.03 |
| 24-48 | 41-86 | 6.41 | 11.73 | 0.15 | 0.10 |
| 48-96 | 46.20 | 66.81 | 37.19 | 2.22 | 0.63 |
| 96-192 | — | 25.63 | 49.59 | 8.02 | 2.73 |
| 192-384 | — | — | — | 89.53 | 19.30 |
| 384-768 | — | — | — | — | 77.20 |
| Basis | Average Pyrite Particle Size, Microns | | | | |
| Area | 47.3 | 77.2 | 166.8 | 275.8 | 522.3 |
| Volume | 54.5 | 78.6 | 171.9 | 278.9 | 534.4 |

The data were processed using the ash diffusion controlled model and the chemical reaction controlled model. For the latter rate expression, dependence on oxygen partial pressure to the 0.7 power was used; for the former the model requires a first order dependence on oxygen partial pressure. The expression for $\tau$ used in the diffusion controlled model is given by Eq. 24; for reaction control

$$\tau = \frac{\rho_B R}{b\, k_{rn}\, C_{AS}^{0.7}} \tag{29}$$

The results showed the reaction controlled model to be better by several measures. The effective diffusivity in the diffusion controlled model exhibited a greater apparent dependence on reaction time and pyrite particle size than did the kinetic rate constant in the reaction controlled model. For all experiments, the relative standard deviation of $D_e$ was greater than for $k_{rn}$. The activation energy for $k_{rn}$ was found to be 35 × $10^3$ kJ/kmol, in agreement with results of other workers in chemically controlled pyrite oxidations. Based on these results Eq. 29 was used for rate expression.

It was necessary to adapt the rate expression for use with coals other than Lower Freeport seam and for coals with a broad distribution of particle sizes such as would be encountered in commercial processing and as were used in the reactions conducted in the continuous bubble column reactor. Reactions

TABLE 3. EXPERIMENTAL DETAILS

| Coal | Lower Freeport | | Upper Freeport | | | Island Creek Western Kentucky | | | Pittsburgh No. 8 | | |
|---|---|---|---|---|---|---|---|---|---|---|---|
| Experiment No. | 1 | 2 | 1 | 2 | 3 | 1 | 2 | 3 | 1 | 2 | 3 |
| Initial heating value kJ/kg (MAF) | 34,966 | 34,966 | 35,239 | 35,239 | 35,239 | 34,032 | 34,032 | 34,032 | 34,180 | 34,180 | 34,180 |
| Initial Sulfur Content, % wt. | | | | | | | | | | | |
| Total | 2.7 | 2.7 | 1.82 | 1.82 | 1.82 | 4.2 | 4.2 | 4.2 | 4.13 | 4.13 | 4.13 |
| Pyritic | 1.93 | 1.93 | 1.16 | 1.16 | 1.16 | 1.96 | 1.96 | 1.96 | 2.27 | 2.27 | 2.27 |
| Organic | 0.58 | 0.58 | 0.6 | 0.6 | 0.6 | 2.15 | 2.15 | 2.15 | 1.66 | 1.66 | 1.66 |
| Sulfate | 0.18 | 0.18 | 0.06 | 0.06 | 0.06 | 0.08 | 0.08 | 0.08 | 0.2 | 0.2 | 0.2 |
| Temperature, °K | 477 | 477 | 453 | 443 | 448 | 452 | 453 | 470 | 441 | 439 | 443 |
| Total presure, MPa | 6.69 | 6.64 | 6.55 | 6.55 | 6.48 | 6.89 | 6.89 | 6.89 | 6.89 | 6.89 | 6.89 |
| Slurry space time (based on total vol.), s | 1860 | 606 | 360 | 1800 | 1800 | 1710 | 1680 | 1760 | 542 | 2643 | 2820 |
| Air flow rate, gmol/s $\times 10^2$ | 0.7 | 2.07 | 1.18 | 0.75 | 0.6 | 0.66 | 2.0 | 1.33 | 1.4 | 0.96 | 0.59 |
| Feed slurry concentration, % wt. | 26 | 26 | 25.9 | 25.9 | 25.9 | 26 | 26 | 26 | 26 | 20 | 20 |
| Product Sulfur Content, % wt. | | | | | | | | | | | |
| Total | 0.91 | 1.18 | 0.87 | 0.77 | 0.73 | 2.8 | 2.5 | 2.4 | 2.9 | 1.93 | 2.58 |
| Pyritic | 0.26 | 0.44 | 0.25 | 0.08 | 0.07 | 0.51 | 0.3 | 0.3 | 0.9 | 0.22 | 0.93 |
| Organic | 0.59 | 0.65 | 0.58 | 0.62 | 0.58 | 2.28 | 2.12 | 1.97 | 1.78 | 1.59 | 1.56 |
| Sulfate | 0.06 | 0.09 | 0.04 | 0.07 | 0.08 | 0.01 | 0.08 | 0.13 | 0.15 | 0.12 | 0.09 |
| Product heating value, kJ/kg (MAF) | 33,569 | 33,380 | 35,030 | 34,797 | 34,122 | 32,790 | 31,624 | 31,291 | 33,487 | 32,368 | 32,564 |

were carried out in the semi-batch stirred autoclave with Lower Freeport and Upper Freeport coals having the broad distribution of particle sizes (called plant grind) used in the continuous reactor tests. Under the assumption that chemical reaction rate was the controlling step, the reaction results were plotted as $1 - (1 - X)^{1/3}$ vs. time to evaluate an average $\tau$ for each coal by extrapolating to $1 - (1 - X)^{1/3} = 0$.

These results are shown in Figure 9. For reactions run in the continuous bubble column reactor at different conditions of temperature and oxygen partial pressure from those shown in Figure 9, values of $\tau$ were corrected according to Eq. 29 and with use of $35 \times 10^3$ kJ/kmol activation energy. For Kentucky No. 9 and Pittsburgh seam coals the values of $\tau$ were calculated from the results on the Lower Freeport coal.

As mentioned, oxydesulfurization reactions conducted in the stirred semi-batch autoclave were shown to have negligible gas absorption resistance. Calculations indicated that this was also the case for operation of the bubble column reactor. Computed volumetric gas absorption coefficients were used with measured rates of consumption of oxygen to show that in all experiments, less than two percent of the overall concentration driving force for oxygen was used to overcome gas absorption resistance. It was therefore possible to consider chemical reaction to be the rate controlling step in the reactions carried out in the bubble column reactor.

### Comparison between Mathematical Model and Experimental Results from Continuous Bubble Column Slurry Reactor

The results of the experiments in the bubble column reactor in the temperature range 430-480°K are summarized in Table 3. It can be seen that the conversion of pyrite increases with increasing temperature and slurry residence time. To compare the experimental results with the predicted values it is necessary to know, in addition to $\tau$, the extent of solid phase backmixing and fractional gas holdup. Gas holdup was estimated using Hughmark's (1967) data. In the range of coal particle sizes used in this work the settling velocity of particles is small enough to assume the extent of backmixing in the liquid and solid phases are practically the same (Kato et al., 1972; Joshi, 1980). The following correlation was used to calculate the dispersion coefficient (Joshi, 1980)

$$D_{SL} = D_S = 0.38 d_p^{1.33}\, g(V_G - \epsilon_G V_{b\infty})^{1/3} \tag{30}$$

The value of average residence time was obtained from the actual slurry volume in the reactor, and the Peclet number for the slurry was calculated from the equation

$$\mathrm{Pe} = \frac{L\, V_{SL}}{(1 - \epsilon_G)\, D_S} \tag{31}$$

The predicted value of conversion can be obtained from Figure 7.

TABLE 4. COMPARISON BETWEEN PREDICTED AND EXPERIMENTAL VALUES OF PYRITE CONVERSION

| Coal | Lower Freeport | | Upper Freeport | | | Island Creek Western Kentucky | | | Pittsburgh No. 8 | | |
|---|---|---|---|---|---|---|---|---|---|---|---|
| Experiment No. | 1 | 2 | 1 | 2 | 3 | 1 | 2 | 3 | 1 | 2 | 3 |
| $\tau$, s | 1162 | 1162 | 1159 | 1400 | 724 | 1794 | 1794 | 1276 | 3090 | 3180 | 3000 |
| $\bar{t}$, s | 1711 | 509 | 317 | 1656 | 1674 | 1590 | 1428 | 1559 | 477 | 2432 | 2651 |
| Pe | 3.1 | 7.26 | 14.3 | 3.15 | 3.26 | 3.5 | 2.7 | 2.8 | 9.2 | 2.0 | 2.2 |
| Predicted fractional conversion | 0.96 | 0.75 | 0.58 | 0.92 | 0.96 | 0.9 | 0.87 | 0.95 | 0.45 | 0.86 | 0.88 |
| Experimental fractional conversion | 0.86 | 0.78 | 0.79 | 0.93 | 0.94 | 0.74 | 0.85 | 0.85 | 0.6 | 0.9 | 0.59 |

Table 4 shows the comparison between the predicted and experimental values of fractional conversion of pyrite. A fairly good agreement is observed. Among limitations of our model in describing reactor performance we note the following. Due to the small column diameter, wall effects could have been significant, even to the point of inducing slug flow instead of bubbly flow. This would give different values for gas void fraction and slurry residence times than were computed. Furthermore a single value of pyrite particle diameter was used in the analysis even though the diameters were in fact distributed.

## CONCLUSIONS

(1) Performance charts for gas-liquid-suspended solids reactors of the continuous (e.g., bubble column) type have been presented. These charts should be useful for the design and scale-up of such reactors.

(2) Experiments in the continuous bubble column slurry reactor indicate that more than 95% of the pyritic sulfur can be removed from the coals tested in the temperature range of 450-475°K, residence time of 1800 s, and Peclet numbers based on solid phase in the range of 2-5.

(3) The experimental results have been compared with the reaction/dispersion model based on the shrinking core mechanism with chemical reaction rate controlling. Fairly good agreement was observed.

## NOTATION

$a$ = effective gas-liquid interfacial area, $m^2/m^3$
$a_p$ = effective liquid-solid interfacial area, $m^2/m^3$
$b$ = stoichiometric coefficient, Eq. 1
$b_r$ = eigenvalues of the Eq. 14
$C$ = dimensionless concentration of the tracer
$C_{in}$ = inlet concentration of the tracer
$c$ = concentration of the tracer
$C_{AC}$ = concentration of dissolved solute gas at the shrinking core surface, $kmol/m^3$
$C_{AI}$ = concentration of dissolved solute gas at the gas-liquid interface, $kmol/m^3$
$C_{AL}$ = concentration of dissolved solute gas in the bulk liquid, $kmol/m^3$
$C_{AS}$ = concentration of dissolved solute gas at the solid surface, $kmol/m^3$
$D$ = axial dispersion coefficient, $m^2/s$
$De$ = effective diffusivity, through product ash layer, $m^2/s$
$d$ = column diameter, m
$E$ = exit age distribution
$g$ = acceleration due to gravity, $m/s^2$
$k_L$ = true gas-liquid mass transfer coefficient, m/s
$k_{rn}$ = $n$th order reaction rate constant, m/s $(kmol/m^3)^{1-n}$
$k_{SL}$ = true liquid-solid mass transfer coefficient, m/s
$k_La$ = volumetric gas-liquid mass transfer coefficient, $s^{-1}$
$k_{SL}a_p$ = volumetric liquid-solid mass transfer coefficient, $s^{-1}$
$L$ = length of the reactor, m
Pe = Peclet number
$p_{O_2}$ = oxygen partial pressure, MPa
$Q$ = amount of the pulse tracer
$R$ = particle radius, m
$R_A$ = volumetric rate of absorption, $kmol/m^3s$
$r_c$ = radius of the shrinking core, m
$T$ = temperature, °K
$T_r$ = eigenvalue, Eq. 16
$t$ = time, s
$\bar{t}$ = average residence time, $L(1 - \epsilon_G)/V_L$, s
$V$ = superficial velocity, m/s
$V_{bx}$ = terminal rise velocity of a single bubble, m/s
$X$ = average fractional conversion
$x$ = fractional conversion
$Z$ = dimensionless axial distance
$z$ = axial coordinate, m

### Greek Letters

$\delta_{SL}$ = liquid film around the particle, m
$\theta$ = dimensionless time, $t/\bar{t}$
$\epsilon$ = fractional holdup
$\rho$ = molar density of pyrite, $kmol/m^3$
$\tau$ = time required for complete conversion, s

### Subscripts

$G$ = gas
$L$ = liquid
$S$ = solid
$SL$ = slurry

## LITERATURE CITED


Biernat, R. J., and R. C. Robins, "High Temperature Potential/pH Diagrams for the Sulfur-Water Systems," *Electrochimica Acta*, **14**, 809 (1969).

Chuang, K. C., M. C. Chem, R. T. Greer, R. Markuszewski, Y. Sun, and T. D. Wheelock, "Pyrite Desulfurization by Wet Oxidation in Alkaline Solutions," *Chem. Eng. Commun.*, **7**, (1-3), 79-84 (1980).

Choudhari, R. V., and P. A. Ramchandran, "Three Phase Slurry Reactors—Journal Review," *AIChE J.*, **26**, 177 (1980).

Govindarao, V. M. H., "On the Dynamics of Bubble Column Slurry Reactors," *Chem. Eng. J.*, **9**, 229 (1975).

Greer, R. T., R. Markuszewski, and T. D. Wheelock, "Characterization of Solid Reaction Products from Wet Oxidation of Pyrite in Coal Using Alkaline Solutions," Scanning Electron Microscopy/1980/I, 541-550.

Hughmark, G. A., "Holdup and Mass Transfer in Bubble Columns," *Ind. Eng. Chem. Process Des. Dev.*, **6**, 218 (1967).

Joshi, J. B., "Axial Mixing in Multiphase Reactors—A Unified Correlation," *Trans. Instn. Chem. Engrs.*, **58**, 155 (1980).

Joshi, J. B., Y. T. Shah, J. A. Ruether, and H. J. Ritz, "Particle Size Effects in Oxidation of Pyrite in Air/Water Chemical Coal Cleaning," AIChE 73rd Annual Meeting, Chicago (1980).

Kato, Y., A. Nishiwaki, T. Fukuda, and S. Tanaka, "The Behavior of Suspended Solid Particles and Liquid in Bubble Columns," *J. Chem. Eng. Japan*, **5**, 112 (1972).

Levenspiel, O., and K. B. Bischoff, "Patterns of Flow in Chemical Process Vessels," *Adv. Chem. Eng.*, **4**, 95-198 (1963).

Levenspiel, O., "Chemical Reaction Engineering," John Wiley & Sons, Inc., New York (1972).

McKay, D. R., and J. Halpern, "A Kinetic Study of the Oxidation of Pyrite in Aqueous Suspension," Trans. Metall. Soc., AIME, **212**, 301 (1958).

Mecklenburgh, J. C., and S. Hartland, "The Theory of Backmixing," John Wiley, New York (1975).

Meyers, R. A., "Coal Desulfurization," Marcel Dekker, Inc., New York (1977).

Narayanan, S., V. K. Bhatia, and D. K. Guha, "Suspension of Solids by Bubble Agitation," *Can. J. Chem. Eng.*, 47-360 (1969).

Parulekar, S., and Y. T. Shah, "Modeling of Three Phase Reactors," *Chem. Eng. J.*, **19** (1980).

Ruether, J. A., "Reaction in a Cascade of Continuous Stirred Tank Reactors of Particles Following the Shrinking Core Model," *Can. J. Chem. Eng.*, **57**, 242 (1979).

Shah, T., "Gas-Liquid-Solid Reactor Design," McGraw-Hill, New York (1979).

Slagle, D., Y. T. Shah, and J. B. Joshi, "Kinetics of Oxydesulfurization of Upper Freeport Coal," *Ind. Eng. Chem. Proc. Des. Dev.*, **29**, 294 (1980).

Vracar, R., and D. Vucurovic, "Oxidation of Pyrites by Gaseous Oxygen from an Aqueous Suspension at Elevated Temperatures in an Autoclave (I)," Technika (Belgrade)—RIM, V. 25, No. 8, 1490-1494 (1970).

Warzinski, R. P., J. A. Ruether, S. Friedman, and F. W. Steffgen, "Proceedings: Symposium on Coal Cleaning to Achieve Energy and Environmental Standards," V-2, EPA 600/7-29-0986, 1016 (1979).



*Manuscript received September 4, 1980; revision received January 14, and accepted January 20, 1981.*